Spontaneous Pupillary Oscillation Signal Analysis Applying Hilbert Huang Transform

Fabiola M. Villalobos-Castaldi[1], José Ruiz-Pinales[2], Nicolás C. Kemper-Valverde[1],
Mercedes Flores-Flores[3], Laura G. Ramírez-Sánchez[1] and Metztli G. Ortiz-Hernández[1]

[1]*Centro de Ciencias Aplicadas y Desarrollo Tecnológico, UNAM, Expert Systems Lab,*
Circuito Exterior S/N C.P. 04510, Ciudad Universitaria, Ciudad de México, D.F., Mexico
[2]*Electronics Engineering Department, Engineering Division, Universidad de Guanajuato*
Carretera Salamanca - Valle de Santiago Km. 3.5 + 1.8. Comunidad de Palo Blanco Salamanca,
Leon, Gto., C.P. 36885, Mexico
[3]*Tecnológico de Estudios Superiores de Ecatepec, Av. Tecnológico S/N, Valle de Anahuac, C.P. 55210,*
Ecatepec de Morelos, Mexico

Abstract: This paper proposes a new application of the Hilbert-Huang transform (HHT). Pupillogram recordings were analyzed through the non-traditional HHT to investigate patterns in the time-frequency parameters of Spontaneous Pupillary Oscillation (SPO) signals. The traditional Fourier transform is only useful for linear stationary signals analysis, but the HHT was designed for the analysis of non-linear and non-stationary signals. However, the HHT is a more suitable tool to study SPO signals which are fundamentally non-stationary. The intrinsic properties of the Spontaneous Pupillary Oscillation signals were highlighted by the HHT scheme and the results showed that SPO waves present local and intermittent variations through the time span. The numerical parameters demonstrated that it is a wide inter-subject variation in the intrinsic time-frequency parameters contribution from each yielding mode to the total signal content.

1 INTRODUCTION

This study proves the assumption that spontaneous pupillary fluctuation is stationary can be a serious misconception. Complex interactions exist between the sympathetic and para-sympathetic systems which are two components of the ANS autonomic nervous system acting as a balance between competing neural mechanisms. Using selected stimulations, the dynamics of this balance mechanism could be significantly altered. Such modifications can be studied using relevant autonomic indices (De Souza, et al., 2007).

The iris is a vascular structure and changes in pupil size are controlled by two smooth muscles in the iris (Sylvain and Brisson, 2014). The sphincter pupillae located in the stromal layer is under cholinergic control, mediated via para-sympathetic nerves from the Edinger-Westphal nucleus. The dilated pupillae situated posterior to the constrictor muscle is innervated by adrenergic fibers originating in the superior sympathetic ganglion. This set of opposing muscles exercise a fine but extensive control over the pupil (Newman, 2008).

The constriction and dilatation of the pupillary aperture is produced mainly through ANS control exerted on the muscles of the iris. More specifically, neurons of the PSN innervate circular fibers of the iris, causing pupillary constriction, whereas excitation by SNS neurons causes the radial fibers of the iris to produce dilation of the pupil (Lowenstein, 1950). Pupil diameter can range from 1.5 to more than 9 millimeters in humans, and a little time, just about 0.2 seconds, it is required by the muscles of the iris to react to stimulation (Goldwater, 1972). The ANS in its role of maintaining homeostasis is in a state of constant fluctuation (Malpas, 2010), (Hreidarsson and Gundersen, 1988). This fluctuation, expressed by spontaneous variations in the rhythmic changes in pupil-size of around 1% occurs with heart beats and

breathing due to fluctuations in blood pressure (Warga, et al, 2009). The variance of normal pupil size is very large. When a constant light level is maintained, the pupil is seen to exhibit continual fluctuations called Spontaneous pupillary fluctuations (SPF) or pupil unrest or physiological hippus. These variations in pupil size is a characteristic of the regulatory mechanism and it is often said that it shows a state of pupillary unrest. This is a physiologic phenomenon that represents a dynamic equilibrium of pupil size of the sympathetic and para-sympathetic activity modulated by the central nervous system is responsible (Newman, 2008), (Nowak et al., 2008). A typical recording of pupil size in a constant light source shows marked spontaneous activity with an irregular pattern of a periodic oscillation. Unrest amplitudes are highest for medium pupil sizes (Rosenberg and Kroll, 1999).

2 RELATED WORKS

In the nighties (McLaren et al., 1992) the authors developed digital filtering techniques and Fourier analysis to calculate several parameters designed to report hippus and miosis. These techniques provided a quantitative manner to evaluate pupillograms to be used in the assessment of alertness. The first parameter designed to report hippus was derived from the Fourier-transformed pupillogram and was the area of the frequency spectrum in a selected band of frequencies. A second parameter to report hippus was also investigated. Spectra differ the most at low frequencies. At higher frequencies, differences were seen to diminish.

A fast Fourier transformation was carried out as a vigilance objective test for frequencies from 0.0 to 0.8 Hz in (Lüdtke et al., 1998) with the purpose of detecting fatigued waves, i.e., slow pupillary oscillations. For temporal changes analysis in the frequency domain of pupillary oscillation two parameters were extracted. One parameter based on the FFT regarded only frequencies below 0.8 Hz, neglecting fast pupillary changes (>1.5625 Hz). An additional parameter referring to the tendency for pupil instability, the pupillary unrest index (PUI), was defined by cumulative changes in pupil size based on mean values of consecutive data sequences. The power and PUI were compared using the Mann–Whitney U-test. Both parameters showed significant differences between the two groups. The main differences between an alert and a sleepy group of people in power and PUI demonstrated the usefulness of this method to objectively detect and quantify sleepiness.

The study purpose reported in (Calcagnini et al, 2000) was to assess whether and the extent LF and HF rhythms contribute to spontaneous pupil diameter fluctuations in rest and during sympathetic activation. To investigate the statistical properties of the SPDF, a parametric spectral and cross-spectral estimation was used. The spectral coherences were used to quantify the statistical link among rhythms in different signals. A rhythmic respiratory component (HF) was clearly found at 0.25 Hz in the pupillogram spectrum in all the subjects. Cross spectral analysis showed a significant coherence in this band between pupil and respiration, pupil and tachogram, and pupil and systogram (Cerutti, 2000).

In conclusion the analysis of the SPF showed the contribution of two specific harmonic components, which have been found to correspond to the well-known LF and HF rhythms of the Heart Rate and Blood Pressure variability signals (Cerutti, 1997). Additionally, the authors concluded that the apparently stochastic behavior of the spontaneous PDF hides specific harmonic components reflecting autonomic activity (Cerutti, 1999).

In the two thousands (Nowak et al, 2008) the authors developed a new method of variability description for the Spontaneous Pupillary Fluctuation (SPF) signals based on the time-frequency analysis by studying the variability of the SPF signal spectrum. The application of fast pupillometry for recording the SPF permitted expanding the analyzed frequency band to 20 Hz. The proposed method of analysis and the introduced measures of SPF variability helped them in the detection and quantitative description of short-lasting time-frequency and time-amplitude variations that were obscured by the overall spectral analysis (Elsenbruch, 2000). The authors mentioned that the Fourier Transform (which requires a stationary signal and is commonly used in the spectral analysis of SPF), has limitations in signal testing. It was concluded that the SPF signal is non-stationary, i.e. its spectrum is varying in time. Thus, it was clearly demonstrated that the previous assumptions are no longer valid (Longtin, 1989).

The previous belief was that fluctuations in pupil diameter arose from random processes, but new results from chaotic time series has shown that they may also arise from deterministic systems (Rosenberg and Kroll, 1999). The accumulated evidence supports the notion that the dynamics of pupil size are governed by deterministic chaos rather than a linear or stochastic process, and this has been demonstrated by analyzing the pupil size versus time from six subjects using pupillography and nonlinear

techniques (Rosenberg and Kroll, 1999). The examined values of the correlation dimension, the Hurst exponent, the flat power spectra, the values of the Lyapunov exponent, and phase plane analyses indicate a chaotic system as the origin of the phenomenon. Pupil activity reported showed repetitive complex patterns which could be explained by a chaos rather than a random system (Rosenberg and Kroll, 1999).

As previously mentioned, the SPF signal analysis has been used for monitoring the level of alertness in clinical conditions, diagnosing sleep disorders, assessing how the different rhythms of the SPS contribute to spontaneous pupil diameter fluctuations at rest and during sympathetic activation, and also for assessing the efficacy of therapeutic interventions (Boyina et al., 2012), (Naber et al., 2013), (Jain et al., 2011), (Heaver, 2012), (Calcagnini et al., 2000), (Bouma and Baghuis, 1971), (Pedrotti et al., 2014), (Regen et al., 2013) and (Lüdtke et al., 1998). These analyses have generally been performed by spectral indices computed from standard spectral analysis techniques (as the Fast Fourier Transform). Such methods have generated comparable results but cannot account for the unavoidable inter-individual variability that naturally occurs in the pupillary fluctuation signals. There are some crucial restrictions using these techniques: the system must be linear and the data must be strictly stationary; otherwise, the features extracted via the Fourier Transform do not have any physiological significance (Boyina et al., 2012), (Cong, Z. 2009).

Ephemeral nature of many physiological events indicates associated data are non-linear and non-stationary waves. Even so, data being non-stationary has not received the proper attention and its effects are frequently disregarded. Serious consequences of such assumptions are inaccurate results or incorrect interpretation of the underlying physics.

Even if under exceptionally general conditions, Fourier transform may be used by those methods, it exists some basic limitations: indeed the system has to be linear and the data must be strictly periodic or stationary. Hence, if conditions are not keep within such limits, then the resulting spectrum will not make any sense physically at all, and Fourier spectral analysis based methods will be considered of limited use. Having no alternatives, current works are still using Fourier spectral analysis to process such data (Huang, N., 2005). (Faust and Bairy, 2012). At the end, methods which do not assume a stationary status (Cong , Z., 2009) are hardly desirable to have.

In the light of such conditions, it is clear that computer methods using Fourier spectral analysis are of limited use. Shortly, both the indiscriminate use of Fourier spectral analysis and the acceptance of the stationary and linearity sates may give wrong results, some of them are described below. (Huang, N., 2005). (Faust and Bairy, 2012). It is desirable to employ quantitative methods which do not assume a stationary status (Cong, Z., 2009). The Hilbert Huang Transform (HHT) initially developed for natural and engineering sciences and now is applied to financial data (Huang et al., 2003). The HHT method is specially developed for analyzing non-linear and non-stationary data.

Nowadays, several methods are available for the time-frequency analysis of non-stationary signals. For instance, the short-time Fourier transformation (STFT) can be used when the signal is piece-wise stationary, whereas the wavelet transform can be used for linear non-stationary signals (Wu and Huang, (2005). One drawback of the wavelet transform is that a *priori* knowledge about the signal to analyze is needed in order to choose a suitable wavelet. Another drawback is that its time-frequency resolution is limited by the Heisenberg-Gabor uncertainty principle. In contrast, the HHT can be used to analyze non-linear and non-stationary signals with excellent resolution in both time and frequency (Barnhart and Eichinger 2011) and (Barnhart, 2011).

3 HILBERT HUANG TRANSFORM

HHT's development was motivated by the need to describe non-linear and non-stationary distorted waves in detail (Huang and Long, 2006). It was designated by the National Aeronautics and Space Administration (NASA) Goddard Space Flight Center (GSFC), and pioneered by (Huang, Long and Shen, 1996), (Huang et al., 1999), (Huang et al., 1998), (Huang et al., 2003), (Huang and Shen, 2005) and (Huang et al., 2007). Since this new analysis technique was developed, it has shown the ability to analyze non-linear and non-stationary data in many areas of research (bio-signal, chemistry, chemical engineering, financial applications and others).

Different from many of the previous transform methods, like Fourier-based techniques [wavelet and fast Fourier Transform], this remarkable method is intuitive, direct, a posteriori, and adaptive; and consequently, highly efficient. Mainly because its origin rise from the decomposition based on and derived from the physical signal. The bases so derived have no close analytic expressions, and they can only

be numerically approximated. (Huang, N. 2005).

This decomposition method is adaptive, and therefore, highly efficient. As indicated by (Flandrin et al., 2004), one of the advantages of the HHT is that its data driven criteria is not fully dependent on theoretical input or formula. Also, the HHT analyzes non-stationary signals locally.

There are two processes involved in the HHT: the Empirical Mode Decomposition (EMD) and the Hilbert Spectral Analysis (HSA). The key part of the method is the pre-processing step, the EMD, in which any complicated data set can be decomposed into a finite and often small number of Intrinsic Mode Functions (IMF). With the Hilbert transform, the IMF yields instantaneous frequencies as functions of time that give sharp identifications of imbedded structures (Huang et al., 2003). The final presentation of the results is a time-frequency-energy distribution, which was designated as the Hilbert Spectrum. Comparisons with the Wavelet and Fourier analyses showing that the HHT method offers much better temporal and frequency resolutions.

The Hilbert transform, $\hat{y}(t)$, of any function or signal $x(t)$ is given by:

$$H[x(t)] \equiv \hat{y}(t) = \frac{1}{\pi} PV \int_{-\infty}^{\infty} \frac{x(t)}{t - \tau} d\tau \qquad (1)$$

where PV denotes the Cauchy's principle value integral.

An analytic representation of the signal can be formed with the Hilbert transform pair as:

$$z(t) = x(t) + i\hat{y}(t) = A(t)e^{i\theta(t)} \qquad (2)$$

where

$$A(t) = (x^2 + \hat{y}^2)^{1/2},$$
$$\theta(t) = tan^{-1}\left(\frac{\hat{y}}{x}\right), \qquad (3)$$
$$\text{and}$$
$$i = \sqrt{-1}$$

$A(t)$ and $\theta(t)$ are the instantaneous amplitudes and phase functions, respectively (Huang et al., 2001). The instantaneous frequency can be computed by means of:

$$\omega = \frac{d\theta(t)}{dt} \qquad (4)$$

In order to apply the Hilbert transform to a signal, it must first be converted to a symmetric signal with mean zero and no negative maxima and no positive minima. The Empirical Mode Decomposition (EMD)

is a method to reduce a signal into a collection of intrinsic mode functions with "well-behaved" Hilbert transforms. Unlike the Fourier series or transform, this representation allows a simultaneous understanding of the signal in both frequency and time.

3.1 Empirical Mode Decomposition

Empirical Mode Decomposition (EMD) is a tool which provides a signal-adaptive decomposition useful for the analysis of non-stationary and non-linear data and shows a strong capability to precisely adjust to the spectral content of the analyzed data. It is based on the concept that any complicated set of data can be decomposed into a finite and often small number of mono-component signals called the Intrinsic Mode Functions (IMF) which are associated with different spectral contributions and then applicable to compute the physical meaning of the complex signal. Decomposition of a signal is made through an iterative process to cancel out the local means from the signal. The sifting process is as follows:

1. Compute all the local extrema (maxima and minima).

2. Obtain the upper envelope by connecting all the local maxima with a cubic spline.

3. Repeat for all the minima to obtain the lower envelope.

Then, the mean of the splines is subtracted from the original signal. The sifting process is repeated with the resulting residual signal until the mean and standard deviation of the average spline is near zero. The resulting residual signal meets the definition of an IMF. An IMF is therefore defined as a signal with zero-mean, and number of extrema and zero-crossings differing by at most one (Huang et al., 1998), (Huang et al., 1999) and (Huang et al., 2003). This first IMF is subtracted from the original signal and the whole sifting process is repeated with this new residual signal. The decomposition process stops when the residue is a monotonic function which not an IMF. The last extracted IMF corresponds to the trend which is the lowest frequency component of the signal.

As a result, the original signal $D(t)$ can be written in terms of the IMFs and the final residue as:

$$D(t) = R_n(t) + \sum_{j=1}^{n} IMF_j(t) \qquad (5)$$

Using equations 2 and 3, the analytic function can be written as:

$$D(t) - R_n(t) = Re\left[\sum_{j=1}^{n} A_j(t)e^{i\int \omega_j(t)dt}\right] \quad (6)$$

This function has a similar form to the Fourier decomposition of a signal $x(t)$:

$$D(t) = Re\left[\sum_{j=1}^{n} A_j e^{i\omega_j t}\right] \quad (7)$$

Thus, the EMD decomposition can be regarded as a generalized Fourier decomposition. Unlike the Fourier transform, which is predicated on a priori selection of basic functions that are either of infinite length or have fixed finite widths, this empirical decomposition method is adaptive, and, therefore, highly efficient (Cong, Z., 2009). Since the decomposition is based on the local characteristic data time scale, it is applicable to non-linear and non-stationary processes. The EMD is also useful as a filter to extract variability of different scales. At a signal time instance, only a single frequency component exists. The EMD method is a necessary data pre-processing before the Hilbert transform can be applied (Huang, N.E., 2003).

4 DATA PROCESSING AND ANALYSIS

A data set of 44 documented pupillary records of healthy university students has been analyzed. Length of signals are one minute at a rate of 30 fps. Details of the collected data are: an IR video camera was used for recording one eye only, typically the left eye, and they were done under constant luminance level (40 cd/m^2). Frame by frame, pupil images were recorded and transferred by means of a video capture board providing real-time digitizing besides the video sequences. The video-capture board was fitted by USB on a Pentium® Dual-Core T4200 @ 2 GHz and 4 GB of internal memory; MATLAB 7.10 (R2013a) was used to obtain real time recordings of the movie. The video sequences were collected from subjects in a resting condition, that is, they were seated on a comfortable chair. Experiment facilities were located in a quiet usability laboratory. For readers going into details about the infrared video Pupillography system and the image processing method, please refer to (Villalobos and Suaste, 2013).

Following the procedure described above (EMD algorithm) the SPO signals were decomposed into their IMF components. To exemplify the results obtained from EMD, in Figure 1 a segment of the IMF components obtained from a selected SPO signal (black line) are shown. In this example, the algorithm yielded 8 components (blue lines) plus a residue R (red line). Each IMF has a distinctive amplitude and frequency content. For the whole data set (44 pupillograms), the number of IMFs needed to decompose the signals fluctuates from 4 to 10 modes (plus the non-linear trend or residue R) Huang et al., indicated that the broad number of modes extracted from a signal is approximately equal to $\log_2 (N)$, where N is the number of points per signal (Huang et al., 2003). The values obtained in this study fall within the limits set by that expression.

The intra signals variations could be due to the informative nature of the IMFs, and is evidence of the numerous and different factors that direct each subject's response. A remarkable advantage of the decomposition is that the local variation of the pupil area can be observed directly, the intrinsic oscillations emerge *naturally* and, based on knowledge of the monitored phenomena, solid conclusions can be obtained about the meaning of each mode and its relationship to particular behaviors.

Even the residue has a sounded meaning; it keeps the mean pupil diameter without fast and short lasting pupil oscillations. The non-linear trend, hallmark of a non-stationary process, is negative because it slowly decays through the time scale (Papoulis and Saunders, 1989). Concerning the frequency and energy levels involved in the residual component, from now on, in the IMFs analysis they will be excluded.

Once the signals were decomposed into their IMFs, a numerical proof of completeness is necessary. The numerical reconstruction of the selected example is as follow:
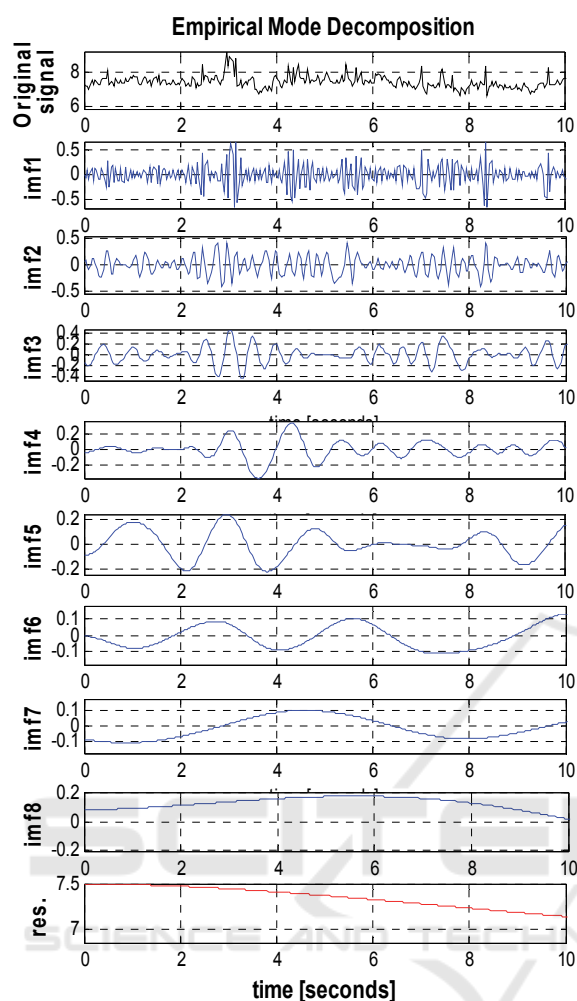
Empirical Mode Decomposition

Figure 1: EMD processing of a typical SPF signal. The top panes is the original signal, imf1 to imf8 are the modes and res is the residue.

Adding R to each component, starting from the longest period component to the shortest (IMF1), the original signal is recreated. When the procedure has reached the IMF2 the original series has been practically recovered (total energy contained in the original SPO data). The latest component (IMF1) does not contribute significantly to reassemble the signal, actually it can be seen as noise. The completeness was numerically verified for the whole data set. The IMFs pertinence was proved through null differences between the original signals and the sum of the components.

4.1 IMF Statistics

In order to clarify the meaning of the IMFs and to use them adequately to describe the studied phenomena, the modes are characterized by well-known statistics metrics.

4.1.1 Period

Based on the definition of the IMF function which established that the frequency of an IMF can change continuously with time, the signal period is assumed as not constant (Huang et al., 2003). The IMF period can be calculated by dividing the number of data points by the number of peaks (local maxima). So, if T is the length of the IMF component and s the number of peaks, then, the IMF period is equal to T/s. A boxplot for the mean period versus IMFs is depicted in Figure 2.
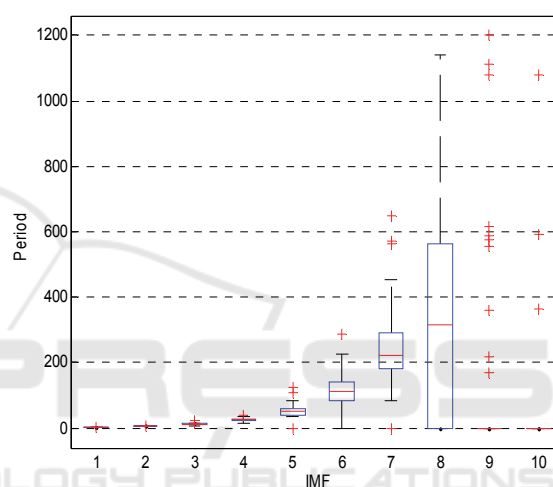

Figure 2: Boxplot for the period content according to the IMF index.

The first mode has the smallest mean period (~3), and for the successive components the mean period doubling is followed. For the last mode, the period variability is evident going from values near zero to the maximum that almost reaches 600 which is indicative of very slow pupillary oscillations. About the period doubling, it is more evident in the first modes and not clearly verified for the last 2 modes; this may be due to the increasingly noticeable presence of noisy components as the decomposition process approaches the residue.

As observed in the graph, there are not significant period differences in the whole data set when analyzing each mode separately. It is important to note that the period significantly changes in the 8th IMF.

4.1.2 Variance

The mean variance contribution from each IMF was

also computed. The variance is used as a simple and intuitively benchmark to determine the significance of each component (IMF) of the original signal. Thus, components with larger variance are more significant.

It was found that the contribution of each IMF to the total variance also changes from signal to signal Figure 3 illustrates the boxplot for the variance contribution (%) depending on the IMF component number.
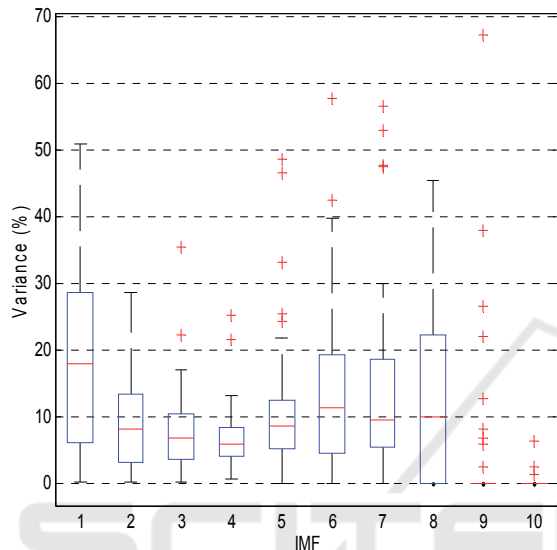

Figure 3: Boxplot for the variance content according to the IMF index.

Table 1: Variance content for a selected subject.

IMF	VAR	VAR (%)	∑ (%)
1	0.0479	31.7013	31.7013
2	0.0305	20.1545	51.8559
3	0.0219	14.4560	66.3119
4	0.0124	8.2111	74.5230
5	0.0089	5.9113	80.4344
6	0.0068	4.4731	84.9074
7	0.0061	4.0455	88.9529
8	0.0167	11.0471	100.0000

Table 1 gives the contribution of each IMF to the total sum of variances for a selected subject in absolute terms, % of total variance and cumulative % variance contribution.

In this table it is possible to see the large differences in the variance contribution from each IMF to the total variance within the selected signals. Based on the variance content reported in Table 1, it is concluded for this specific subject, that the most important components are the highest frequency modes (IMF1, 2 and 3); the sum of variances for these

important components contribute 66.31% of the total variance, but the low frequency components have less effect on the whole change of this SPO signal. The variance intervals of the first components are wide and grow as the mode index increases.

Conversely to the last case, in the SPO wave presented in Table 2, the most important IMF components are the lowest frequency modes (IMF4, 5 and 6), and their variance sum contributes 86.5874% of the total variance. Therefore, the high frequency components have less effect on the total variance of the signal. The interval of the higher frequency components is narrow while the interval of the lower frequency modes becomes wider.

Table 2: Variance content of another selected subject.

IMF	VAR	VAR (%)	∑ (%)
1	0.0007	3.7769	3.7769
2	0.0004	1.9960	5.7729
3	0.0014	7.6397	13.4126
4	0.0038	21.4697	34.8822
5	0.0083	46.6456	81.5279
6	0.0033	18.4721	100.000

As can be concluded, the frequency at which the highest variance contribution occurs changes from signal to signal, so the highest variance content for each signal is present on different IMFs.

4.2 Instant Amplitude and Frequency Analysis

Having obtained the IMF components, it is not difficult to apply the Hilbert transform to each IMF component in order to compute the instantaneous amplitude and frequency according to equation 3 and 4. The combination of the EMD and the Hilbert Spectral Analysis is designated as the Hilbert–Huang Transform (HHT).

4.2.1 Instant Amplitude

Figure 4 shows the boxplot of the amplitude contribution according to the number of IMFs. As can be seen, there is a large variation between components and they are highly intermittent through the time span. The amplitude variation between modes leads to the conclusion that for the studied phenomenon and analyzed population a particular IMF cannot be selected as the one that contains the higher energy levels. The mean amplitude contribution of all components is in the 0.1-0.2 mm interval.

The amplitude has a slight tendency to decrease as

the number of IMFs increases. However, in the first and last modes (8th IMF, which is the most representative before reaching R) the fluctuations of the pupil area are wider (~0 - 0.3mm). The amplitude intervals of in-between modes become high and are mainly concentrated below the ~0.25 mm range. It is evident that there is a wide inter-subject variation and no major modes are detected, i.e. the highest amplitude values for each signal (subject) are on different IMFs. While for some subjects the amplitude is higher at the first modes, for others the maximum values are present at superior.
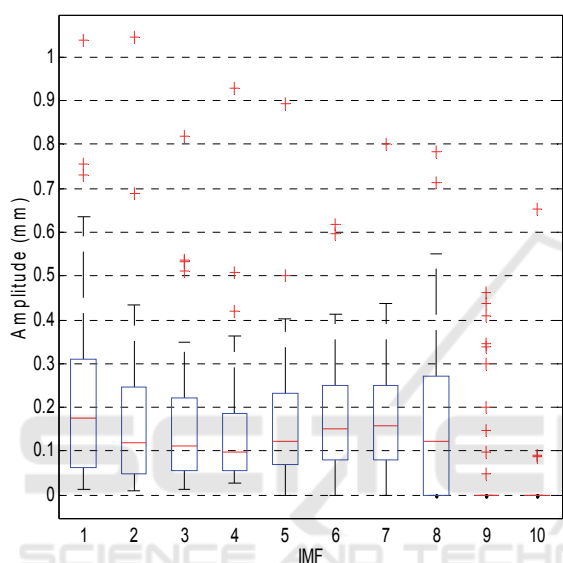
intervals become narrower as the IMF index is higher.

The first mode has the highest frequency content (~ 9 Hz to ~11 Hz), the 2nd IMF frequency is around 5 Hz while from the 3rd to 8th modes the activated frequencies go from ~3 Hz to ~ 0.01 Hz. Observing the response trends defined concerning amplitude behavior, interesting relationships can be pronounced.

There are subjects with strong pupillary oscillations at the first modes; at the highest frequency levels, others present them at the higher modes and at the lower frequency levels.
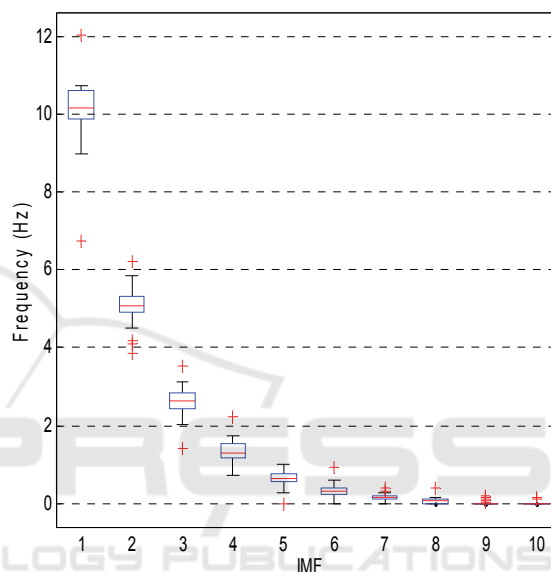

Figure 4: Boxplot for the amplitude content according to the IMF index.

Figure 5: Boxplot for the frequency content according to the IMF index.

There are interesting responses to be noted:

a) Where amplitude levels are almost equally distributed in all modes,
b) Where amplitude values different from zero are only present in the first modes, 1st to 4th IMFs and,
c) Where the amplitude concentration cannot be referred to trends a) nor b).

4.2.2 Frequency

Figure 5 illustrates the boxplot of the frequency variation according to number of IMFs. As can be observed, the frequency value progressively falls as the mode number increases. The frequency range of each IMF is well defined and independent of others. There are marked differences between the limits of the frequency characteristic of each mode. It is verified that the highest frequencies are contained in the first components and, consequently, the latest modes have the lower frequency levels. The variation

With regard to the highlighted responses:

a) Some subjects respond with similar amplitude levels at every frequency detected,
b) The behavior of the subjects having zero amplitudes in the higher modes must be interpreted as responses only in the highest frequency levels and,
c) Some individuals have reactions that activate frequencies below 1 Hz.

The differences in the frequency content and their association with the amplitude has an clear effect on the conclusions about the studied phenomenon, the stationary statement (signals) and even on the classification system that generates the data as nonlinear.

4.3 Spectral Analysis

Having obtained the IMF components, the next step

in the proposed method is to apply the Hilbert Transform to each component and generate the Hilbert Spectrum (HS). Having the Hilbert Spectrum defined, we can compute the Marginal Spectrum (MS) that offers a measure of total amplitude (or energy) contribution from each frequency value. In other words, the MS represents the cumulated amplitude over the entire data spam. So the MS is the HS that was integrated through all time. In this simplification, the time coordination is lost as in the Fourier spectral analysis, which leave a summary of the frequency content of the event.

The frequency in either HS or MS has a completely different meaning from results generated by applying Fourier spectral analysis. The existence of energy at a particular frequency in the Fourier representation, means a component of a sine or a cosine wave persisted through the time span of the data. So the existence of energy at the particular frequency, means only that, in the whole time span of the data, that there is a higher like hood for such a wave to have appeared locally.

In order to try to compare the proposed spectral representation method against Fourier conventional method, we performed a standard FT analysis. In Figure 6 we directly compare the obtained MS (solid line) against the conventional Fourier technique (dotted line) of the SPO data from the Figure 1.
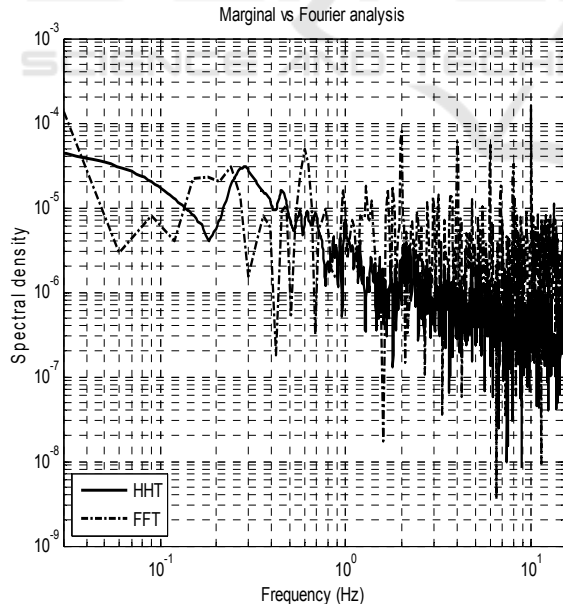

Figure 6: Power spectra of SPF data.

It can be seen that the Marginal spectrum differs from the Fourier based spectrum in two main issues. Although the spectral density at the low-frequency portion is higher in the Hilbert spectra, the Fourier spectrum is dominated by the DC term due to the non-zero mean pupil area, this is also meaningless because of the non-stationary of the data. The spectral density is lower than the Fourier analysis at higher frequencies, which was expected because of the different interpretation of the HHT's and the Fourier-based method of data non-linearity. Most of the Fourier-based techniques always decompose a nonlinear signal into its base frequency and higher harmonics; because of this some spectral energy in the higher frequencies is leaked from their lower frequency sub harmonics. The HHT interprets signal non-linearity in terms of frequency modulation, and the spectral energy of a nonlinear signal remains at the neighborhood of the base frequency (see Figure 6).

These findings coincided with the ones reported by (Nowak et al.2008), where by the application of fast pupillometry for recording and extended spectral analysis in examining SPO signals, they found interesting frequency components in some subjects in the range above 1 Hz. They also reported the existence of several harmonics even up to 20 Hz frequency range. The analysis they carried out showed that the distribution of the PSD amplitude peaks was different for different frequencies.

Contrary to their proposed method where they considered the computed numerical parameters as global, we represent the pupil area fluctuation tacking advantage of the instantaneous frequency approach, which even under the worst conditions, is still consistent with the physics of the system being studied and could represent it much more accurately than previous techniques based on Fourier analysis.

5 CONCLUSIONS

This paper has addressed to the possibility of characterizing the natural behavior of Spontaneous Pupillary Oscillation SPO records by the time-frequency signal variations. The objective of describing data from non-traditional perspectives (time-frequency-intensity domain) and for finding specific and indicative behavior patterns is addressed by applying the HHT to the SPO waves. Non-linear and non-stationary intrinsic characteristics of these signals are discovered and reported in this paper using the advantageous non-traditional signal processing technique.

The EMD was implemented to decompose the original SPO signals; the obtained IMF modes varying from 4-10 plus a non-linear trend which also

showed a clear non-stationary behavior. The fact that the EMD analysis decomposed the spatially distributed SPO data into a set of *natural* oscillations (Khademul, 2006), showed the IMFs are more effective in isolating physical processes of various time scales and are also statistically significant.

The obtained results, lead us to observe that the SPO signals present local and intermittent pupil area variations in time. The EMD successively extracts the IMFs starting with the highest local spatial frequencies in a recursively way, which is effectively a set of successive low-pass spatial filters based entirely on the properties exhibited by the data (Khademul, 2006). It is also observed that there are wide inter-subject differences in the variance, period, amplitude, and frequency contribution from each mode to the total signal. These inter-mode variations, lead us to the conclusion that for the studied phenomenon and analyzed population, a particular IMF cannot be selected as the one that contains the higher amplitude level or dominant frequencies.

Our characterized analysis is of a preliminary nature and many issues have to be addressed and investigated rigorously, and from the obtained results, the HHT seems to have much more potential for this initial approach. Applying non-traditional alternatives to the study of the pupillograms presents a great opportunity to understand behaviors and to mitigate diseases or specific medical conditions, for example: discern between well and diseased states, explore if SPF records could provide information for the evaluation of the psychophysiological response of ANS to affective triggering events or as a quantitative way in the assessment of alertness.

As the SPO signals are not stationary, the Fourier spectrum is meaningless physically, in contrast, we have demonstrated that with the HHT as analytic method, the resulting frequency-energy spectrum provides a physical meaningful interpretation of the signal.

REFERENCES

Barnhart, B. and Eichinger, W., (2011). Empirical Mode Decomposition applied to solar irradiance, global temperature, sunspot number, and CO2 concentration data. Journal of Atmospheric and Solar-Terrestrial Physics, 73(13), pp.1771-1779.

Barnhart, B.L., (2011). The Hilbert-Huang Transform: theory, applications, development, PhD thesis, University of Iowa.

Bouma, H., and Baghuis, L., (1971). Hippus of the pupil: Periods of slow oscillations of unknown origin. Vision Research, 11(11), 1345-1351.

Boyina,S.R, Anu.H, Moneca.K, Mahalakshmi Malini.G, Priyadharshini.R, (2012). Pupil Recognition Using Wavelet And Fuzzy Linear Discriminant Analysis For Authentication, International Journal Of Advanced Engineering Technology, IJAET/Vol.III/ Issue II.

Calcagnini, G., Censi, F., Lino, S., and Cerutti, S., (2000). Spontaneous fluctuations of human pupil reflect central autonomic rhythms. Methods Inf Med, 39(2), 142-145.

Cerutti, S., (1997). Cardiovascular autonomic rhythms in spontaneous pupil fluctuations, Computers in Cardiology 1997 CIC-97.

Cerutti, S., (1999). Baroceptor-sensitive fluctuations of human pupil diameter", Computers in Cardiology,Vol 26 (Cat No 99CH37004) CIC-99.

Cerutti, S., (2000). Pupil diameter variability in humans, Proceedings of the 22nd Annual InternationalConference of the IEEE Engineering in Medicine and Biology Society (Cat No 00CH37143) IEMBS-00.

Cong, Z., (2009). Hilbert-Huang transform based physiological signals analysis for emotion recognition, 2009 IEEE International Symposium on Signal Processing and Information Technology (ISSPIT), 12.

De Souza Neto, E., Abry, P., Loiseau, P., Cejka, J., Custaud, M., Frutoso, J., Gharib, C. and Flandrin, P. (2007). Empirical mode decomposition to assess cardiovascular autonomic control in rats. Fundam Clin Pharmacol, 21(5), pp.481-496.

Elsenbruch, S., (2000). Physiological Measurement, 05.

Faust, O. and Bairy, M., (2012). Nonlinear analysis of physiological signals: a review. J. Mech. Med. Biol., 12(04), p.1240015.

Flandrin, P., Rilling, G., and Goncalves, P., (2004). Empirical mode decomposition as a filter bank. Signal Processing Letters, IEEE, 11(2), 112-114.

Goldwater, B., (1972). Psychological significance of pupillary movements. Psychological Bulletin, 77(5), pp.340-355.

Heaver, B., (2012). Psychophysiological indices of recognition memory (Doctoral dissertation, University of Sussex).

Hreidarsson, A. B., and Gundersen, H. J. G., (1988).Reduced Pupillary Unrest: Autonomic Nervous System Abnormality in Diabetes Mellitus, Diabetes.

Huang, N. (2005). Empirical mode decomposition for analyzing acoustical signals. The Journal of the Acoustical Society Of America, 118(2), 593. http://dx.doi.org/10.1121/1.2040268.

Huang, N. E., and Shen, S. S., (2005). Hilbert-Huang transform and its applications (Vol. 5). World Scientific.

Huang, N. E., Long, S. R., and Shen, Z., (1996). The mechanism for frequency downshift in nonlinear wave evolution. Advances in applied mechanics, 32, 59-117C.

Huang, N. E., Shen, Z., and Long, S. R., (1999). A new view of nonlinear water waves: The Hilbert Spectrum 1. Annual review of fluid mechanics, 31(1), 417-457.

Huang, N. E., Shen, Z., Long, S. R., Wu, M. C., Shih, H. H., Zheng, Q. and Liu, H. H.,(1998). The

empirical mode decomposition and the Hilbert spectrum for nonlinear and non-stationary time series analysis. Proceedings of the Royal Society of London Mathematical, Physical and Engineering Sciences (Vol. 454, No. 1971, pp. 903-995). The Royal Society.

Huang, N., Wu, M., Qu, W., Long, S., and Shen, S., (2003). Applications of Hilbert-Huang transform to non-stationary financial time series analysis. Appl. Stochastic Models Bus. Ind., 19(3), 245-268.

Huang, N.E., and Long, S., (2006). On the Normalized Hilbert Transform and Its Applications in Remote Sensing, Signal and Image Processing for Remote Sensing.

Huang, N.E., (2003). Applications of Hilbert-Huang transform to non-stationary financial time series analysis, Applied Stochastic Models in Business and Industry, 7.

Huang, Y., Schmitt, F. G., Lu, Z., and Liu, Y.,(2007). Empirical mode decomposition analysis of experimental homogeneous turbulence time series. In 21° Colloque GRETSI, Troyes, FRA, 11-14 septembre 2007. GRETSI, Groupe d'Etudes du Traitement du Signal et des Images.

Jain, S., Siegle, G., Gu, C., Moore, C., Ivanco, L., Studenski, S., Greenamyre, J. and Steinhauer, S., (2011).Pupillary unrest correlates with arousal symptoms and motor signs in Parkinson disease. Movement Disorders, 26(7), pp.1344-1347.

Khademul, I.M., (2006)."Empirical mode decomposition analysis of climate changes with special reference to rainfall data", Discrete Dynamics in Nature and Society.

Longtin, A., (1989). Nonlinear Oscillations, Noise and Chaos in Neural Delayed Feedback department of Piysics, McGill University, Montréal, Canada.

Lowenstein, O., (1950). Role of Sympathetic and Parasympathetic Systems in Reflex Dilatation of the Pupil. Archives of Neurology and Psychiatry, 64(3), 313.

Lüdtke, H., Wilhelm, B., Adler, M., Schaeffel, F., and Wilhelm, H., (1998). Mathematical procedures in data recording and processing of pupillary fatigue waves. Vision Research, 38(19), 2889-2896.

Malpas, S., (2010). Sympathetic Nervous System Overactivity and Its Role in the Development of Cardiovascular Disease. Physiological Reviews, 90(2), pp.513-557.

McLaren, J. W., Erie, J. C., and Brubaker, R. F., (1992). Computerized analysis of pupillograms in studies of alertness. Invest. Ophthalmol. Vis. Sci, 33(3), 671-676.

Naber, M., Alvarez, G., and Nakayama, K., (2013). Tracking the allocation of attention using human pupillary oscillations. Frontiers in Psychology, 4.

Newman, S., (2008). Clinical Neuro-Ophthalmology. A Practical Guide. Journal of Neuro-Ophthalmology, 28(4), p.362.

Nowak, W., Hachol, A. and Kasprzak, H., (2008). Time-frequency analysis of spontaneous fluctuation of the pupil size of the human eye. Optica Applicata, XXXVIII, No. 2, pp.269-280.

Papoulis, A., and Saunders, H., (1989). Probability, Random Variables and Stochastic Processes (2nd Edition). J. Vib. Acoust. 111(1), 123.

Pedrotti, M., Mirzaei, M., Tedesco, A., Chardonnet, J., Mérienne, F., Benedetto, S., and Baccino, T., (2014).Automatic Stress Classification with Pupil Diameter Analysis. International Journal of Human-Computer Interaction, 30(3), 220-236.

Regen, F., Dorn, H., and Danker-Hopfe, H., (2013). Association between pupillary unrest index and waking electroencephalogram activity in sleep-deprived healthy adults. Sleep Medicine, 14(9), 902-912.

Rosenberg, M. L., and Kroll, M. H., (1999). Pupillary hippus: an unrecognized example of biologic chaos. Journal of Biological Systems, 7(01), 85-94.

Sylvain, S., and Brisson,J., (2014). "Pupillometry: Pupillometry", Wiley Interdisciplinary Reviews Cognitive Science.

Villalobos-Castaldi, F., and Suaste-Gómez, E. (2013). A new spontaneous pupillary oscillation-based verification system. Expert Systems with Applications, 40(13), 5352-5362. http://dx.doi.org/10.1016/j.eswa.2013.03.042.

Warga, M., Lüdtke, H., Wilhelm, H., and Wilhelm, B., (2009). How do spontaneous pupillary oscillations in light relate to light intensity? Vision research, 49(3), 295-300.

Wu, Z. and Huang, N.E., (2005).Statistical Significance Test of Intrinsic Mode Functions", Interdisciplinary Mathematical Sciences.